APPLIED AND ENVIRONMENTAL MICROBIOLOGY, Oct. 2003, p.6257-6263 Vol. 69, No. 10
0099-2240/03/$08.00+0 DOI: 10.1128/AEM.69.10.6257–6263.2003

A Novel Extracellular Multicopper Oxidase from *Phanerochaete chrysosporium* with Ferroxidase Activity

Luis F. Larrondo,[1] Loreto Salas,[1] Francisco Melo,[1] Rafael Vicuña,[1]* and Daniel Cullen[2]

Departamento de Genética Molecular y Microbiología, Facultad de Ciencias Biológicas, Pontificia Universidad Católica de Chile, Santiago, Chile,[1] and Millenium Institute for Fundamental and Applied Biology, USDA Forest Products Laboratory, Madison, Wisconsin 53705[2]

Received 21 April 2003/Accepted 15 July 2003

Lignin degradation by the white rot basidiomycete *Phanerochaete chrysosporium* involves various extracellular oxidative enzymes, including lignin peroxidase, manganese peroxidase, and a peroxide-generating enzyme, glyoxal oxidase. Recent studies have suggested that laccases also may be produced by this fungus, but these conclusions have been controversial. We identified four sequences related to laccases and ferroxidases (Fet3) in a search of the publicly available *P. chrysosporium* database. One gene, designated *mco1*, has a typical eukaryotic secretion signal and is transcribed in defined media and in colonized wood. Structural analysis and multiple alignments identified residues common to laccase and Fet3 sequences. A recombinant MCO1 (rMCO1) protein expressed in *Aspergillus nidulans* had a molecular mass of 78 kDa, as determined by sodium dodecyl sulfate-polyacrylamide gel electrophoresis, and the copper I-type center was confirmed by the UV-visible spectrum. rMCO1 oxidized various compounds, including 2,2′-azino(bis-3-ethylbenzthiazoline-6-sulfonate) (ABTS) and aromatic amines, although phenolic compounds were poor substrates. The best substrate was Fe^{2+}, with a K_m close to 2 μM. Collectively, these results suggest that the *P. chrysosporium* genome does not encode a typical laccase but rather encodes a unique extracellular multicopper oxidase with strong ferroxidase activity.

Lignin provides the protective matrix surrounding the cellulose microfibrils of plant cell walls. This compound is second only to cellulose in abundance, and its biodegradation is a key step in the carbon cycle. This amorphous and insoluble polymer lacks stereoregularity and, in contrast to cellulose and hemicellulose, is not susceptible to hydrolytic attack (16). White rot fungi are the only known microbes capable of efficient depolymerization and mineralization of lignin (6).

In culture, white rot fungi secrete an array of peroxidases and phenol oxidases. These enzymes act nonspecifically via the generation of lignin free radicals, which undergo spontaneous cleavage reactions (28). Lignin peroxidase (LiP) oxidizes phenolic and nonphenolic substrates by one electron, whereas manganese peroxidase (MnP) oxidizes Mn^{2+} to Mn^{3+}. The latter enzyme, chelated by organic acids produced by the fungus, oxidizes phenolic residues to phenoxy radicals (21, 22, 26, 41). Both peroxidases proceed through the conventional peroxidase cycle, which involves the so-called compound I, compound II, and resting enzyme (34, 46, 47).

Blue copper phenol oxidases, also known as laccases, represent a third type of enzyme activity implicated in lignin degradation (44). Laccases catalyze the one-electron oxidation of phenols, aromatic amines, and other electron-rich substrates with the concomitant four-electron reduction of O_2 to $2H_2O$. Laccases belong to a large family of multicopper oxidases (MCOs) that also includes ascorbate oxidase, Fet3 ferroxidases, and ceruloplasmin. Only two family members, fungal Fet3 (1) and vertebrate ceruloplasmin (49), efficiently oxidize ferrous ions.

The involvement of laccase in ligninolysis is well established in *Pycnoporus cinnabarinus*, a fungus that lacks LiP and MnP (15). Dozens of closely related laccase genes have been characterized from several lignin-degrading fungi. However, some white rot fungi appear not to produce laccase, suggesting that this enzyme may not be essential for lignin decay (23). For decades, the most intensively studied white rot fungus, *Phanerochaete chrysosporium*, was thought to belong to this group (16, 23, 28, 44). Recently, however, laccase activity was detected in *P. chrysosporium* cultures grown under certain conditions (13, 39, 42), but these results have not been widely accepted (37).

In an attempt to resolve the issue of laccase activity in *P. chrysosporium*, we searched the publicly available genome database (www.jgi.doe.gov/programs/whiterot.htm) for laccase-encoding sequences. Four clustered MCO-encoding sequences (*mco1* to *mco4*) were identified, but none corresponded to a sequence encoding a conventional laccase. Structural analysis and heterologous expression of *mco1* support the hypothesis that there is a new branch in the MCO family distinct from fungal laccases.

MATERIALS AND METHODS

Strains. *P. chrysosporium* homokaryotic strain RP-78 and dikaryotic strain BKM-F-1767 were obtained from the Center for Mycology Research, Forest Products Laboratory, Madison, Wis. *Aspergillus nidulans* A122 (*pyrG89 pabaA1 fwA1 ua Y9*) was obtained from the Fungal Genetic Stock Center (Kansas City, Kans.).

cDNA cloning and analysis. Poly(A) RNA from *P. chrysosporium* was extracted from colonized wood chips and from mycelium grown in defined media containing wood-derived crystalline cellulose (Avicel PH-101; Fluka Chemika, Buchs, Switzerland) as the sole carbon source. *mco1* cDNA was obtained by reverse transcription (RT)-PCR of RNA purified from day 6 cultures of

* Corresponding author. Mailing address: Departamento de Genética Molecular y Microbiología, Facultad de Ciencias Biológicas, Pontificia Universidad Católica de Chile, P.O. Box 114-D, Santiago, Chile. Phone: 562-6862663. Fax: 562-2225515. E-mail: rvicuna@genes.bio.puc.cl.

P. chrysosporium grown on Avicel medium (51). RT-PCR amplification of *mco1* cDNA was primed with oligonucleotides flanking predicted translational start and stop codons (45 nucleotides upstream, 5′-CCCATCCTTCACTTTGCATT A-3′; 47 nucleotides downstream, 5′-AAGCGGCACCGAGGCTGGTA-3′). RT-PCR was conducted as described previously (19, 51), with slight modifications. The RT reaction was conducted by using Moloney murine leukemia virus reverse transcriptase (Invitrogen, Carlsbad, Calif.) for 45 min at 42°C. The PCR was performed for only 27 cycles by using high-fidelity polymerase (*Pfu*; Stratagene, La Jolla, Calif.). Nucleotide sequences were determined with an ABI Prism Big Dye terminator cycle sequencing kit (Perkin-Elmer Applied Biosystems, Foster City, Calif.) and ABI automated sequencers. The nucleotide sequence of the *mco1A* gene is available at www.jgi.doe.gov/programs/whiterot.htm and lies on scaffold number 56 between coordinates 152,341 and 155,044.

Multiple-sequence analysis. All multiple-sequence alignments were constructed by using the command MALIGN in the MODELLER software, version 6v1 (www.salilab.org/modeller/modeller.html) (40). Default gap opening and extension penalties of −500 and −100 were used to construct all the initial alignments. The final optimal values were obtained by refinement through an iterative process of alignment and manual inspection of the output, verifying that the highly conserved residues of MCOs involved in copper binding, which are spread over the sequence, were properly aligned. In the case of alignments of two or more blocks of sequences, more permissive values were used.

Structural comparisons. The optimal structural alignment of known protein structures was obtained by using the command MALIGN3D in the MODELLER software, version 6v1 (40), with gap opening and extension penalties of 1.5 and 4.0, respectively. Based on this initial structural alignment, the protein structures were optimally superimposed in three-dimensional space by using the a-carbons of the main chain and the command SUPERPOSE in the MODELLER software. After superimposition of the structures, the final optimal structural alignment was obtained, in which two residues were considered structurally equivalent (or aligned) if the Ca-Ca distance between them in three-dimensional space was less than 4.0 Å.

Dendrogram construction. All dendrograms were constructed from multiple-sequence alignment data. The command ID−TABLE in the MODELLER software, version 6v1 (40), was used to calculate the pairwise sequence identity distance matrix for all sequences in the multiple alignment. The distance matrix was analyzed by using the program *cluster*, version 1.03, of Peter Kleiweg (http://odur.let.rug.nl/~kleiweg/clustering/clustering.html) to construct the dendrogram. The clustering algorithm used was the group average method with Euclidean distance.

Plasmids, genetic construction, and transformation. The *mco1* expression vector (pEXPmco1) was constructed by overlap extension (24). The expression cassette included the *Aspergillus oryrae* TAKA amylase promoter fused to the entire *mco1B* cDNA coding region (with signal sequence) followed by a 199-bp fragment containing the glucoamylase terminator from *Aspergillus awamori* (27). The selectable marker, *pyrG*, was obtained from the Fungal Genetics Stock Center. Cotransformation of *A. nidulans* A722 with pEXmco1 and *pyrG* was performed as described previously (31).

Five hundred milliliters of *Aspergillus* minimal medium containing 5% maltose (31) was inoculated with 10^7 spores ml^{-1} and incubated for 3 days at 30°C in an orbital shaker (125 rpm). Alternatively, transformants were grown in medium containing 0.5% yeast extract and 5% maltose.

Enzyme purification and analysis. Following filtration through Miracloth (Calbiochem Inc., La Jolla, Calif.), 1 liter of day 3 culture medium of *A. nidulans* was concentrated 10-fold by filtration in a 185-ml Amicon cell with a 10-kDa-cutoff membrane. The concentrate was dialyzed twice against 500 ml of 25 mM sodium acetate (pH 4.5) and loaded onto a Q-Sepharose column (1.75 cm^2 by 18 cm) equilibrated with the same buffer (33). The protein was eluted with a 250-ml linear gradient of 50 to 350 mM NaCl dissolved in 25 mM sodium acetate (pH 4.5); 1.8-ml fractions were collected. Recombinant MCO1 (rMCO1) eluted at 100 mM NaCl. Active fractions were pooled and concentrated by dialysis against solid polyethylene glycol 35,000.

Enzyme activity was measured at 30°C with a Shimadzu (Kyoto, Japan) 160 UV-visible recording spectrophotometer. To determine laccase activity, 2,2′-azinobis(3-ethylbenzthiazoline-6-sulfonate) (ABTS) was used as the substrate. Standard reaction mixtures (1.0 ml) contained 4.33 mM ABTS (Sigma) in 100 mM glycine (pH 3.0) as the buffer. One unit was defined as the amount of enzyme required to oxidize 1.0 μmol of ABTS per min. As indicated below, other compounds were also tested as substrates. Ferroxidase activity (oxidation of Fe^{2+} to Fe^{3+}), was monitored spectrophotometrically at 315 nm (De = 2,200 M^{-1} cm^{-1}) (9). A YSI model 53 oxygen monitor fitted with a Gilson single-port 1.8-ml reaction chamber was used to measure oxygen consumption. (For comparative purposes, parallel studies were conducted with recombinant laccase from the basidiomycete *Ceriporiopsis subvermispora* [rLcs1] expressed in *A. niduluns* [30] and with commercial laccase 51002 [Novozymes, Bagsvaerd, Denmark].) Except as indicated below, all oxidase assays were conducted in 100 mM sodium acetate buffer (pH 5.0).

Zymograms obtained by using sodium dodecyl sulfate (SDS)-polyacrylamide gel electrophoresis were prepared as described by Laemmli (29). Samples were applied in nonreducing denaturing loading buffer without boiling and were electrophoresed at 4°C. Gels were fixed in a solution containing 10% acetic acid and 40% methanol for 10 min and then incubated at room temperature in 100 mM glycine buffer (pH 3.0) containing 4.33 mM ABTS or in 100 mM sodium acetate buffer (pH 5.0) containing 1 mM *o*-dianisidine for 10 min. For ferroxidase activity, gels were directly incubated in 0.5 mM Fe^{2+} in 100 mM acetate buffer (pH 5.0) for 20 min and then incubated in a new solution consisting of the same buffer and 0.25 mM batophenanthroline-disulfonic acid for 10 min.

Nucleotide sequence accession number. The *mco1B* cDNA sequence has been deposited in the GenBank database under accession number AY225437.

RESULTS

Identification and characterization of *mco1*. Blast analysis of the *P. chrysosporium* genome (http://www.jgi.doe.gov/programs/whiterot.htm) resulted in identification of four sequences distantly related to laccases (<31% amino acid identity). For pairwise comparisons of the four putative MCOs, the levels of amino acid identity ranged from 52 to 78%, but only *mco1A* had a typical eukaryotic secretion sequence, as predicted by SignalP (http://www.cbs.dtu.dk/services/SignalP). Primers were designed based on this sequence, and a cDNA was obtained following RT-PCR amplification of RNA from *P. chrysosporium* BKM-F1767 grown for 6 days on Avicel medium. The cDNA (GenBank accession number AY225437) corresponds to the allelic version of *mco1A*. The *mco1B* cDNA also was RT-PCR amplified from 2-week-old wood chip cultures (45), and its identity was established by direct sequencing. The allelic cDNAs and proteins are 99.2 and 99.3% identical at the nucleotide and amino acid levels, respectively. Comparison of cDNA and genomic sequences resulted in identification of 19 introns. Both *mco1* alleles encode a 559-amino-acid protein that has a putative 16-amino-acid leader sequence. The deduced mature protein has a predicted molecular mass of 59.1 kDa and a pI of 4.58. BlastP searches of public databases showed that MCO1B is most closely related to *Arxula adeninivorans* ferroxidase (32% identity), followed by laccases from *Coriolus versicolor* and *Trametes villosa* (31%). Cladistic analysis placed MCO1 in the ferroxidase family, not in the laccase family (data not shown).

Structural comparison of MCOs. To help clarify the unusual structural features of MCO1, we analyzed the nonredundant known structures of MCOs. *Coprinus cinereus* laccase (Protein Data Bank [PDB] code 1A65 [14]), *Melanocurpus albomyces* laccase (PDB code 1GW0 [20]), *Trametes versicolor* laccase I (PDB code 1GYC [36]), *T. versicolor* laccase III (PDB code 1KYA [5]), and ascorbate oxidase from *Cucurbita pepo* (zucchini) (PDB code 1AOZ [35]) were optimally superimposed in three-dimensional space, and this analysis revealed 403 structurally equivalent positions with a total root mean square deviation over these positions of less than 1.5 Å. At these positions, 72 identical residues were conserved in all of the structures. Multiple-sequence alignments of ascorbate oxidases and laccases, including MCO1, showed that there were 41 conserved positions, 13 of which were directly involved in the binding of copper (data not shown). Most of these residues were glycines, prolines, or aromatic and

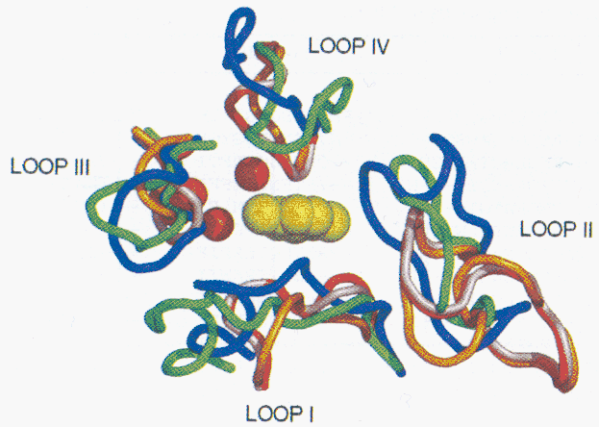

FIG. 1. Structural superimposition of MCO loops involved in substrate binding. Three-dimensional superimposition of *T. versicolor* 1KYA (red), *T. versicolor* 1GYC (pink), *C. cinereus* 1A65 (orange), and *M. albomyces* IGWO (blue) laccases and zucchini 1GYC ascorbate oxidase (green) is described in Materials and Methods.

charged residues. Unfortunately, Fet3 could not be included in this comparative analysis due to a lack of crystallographic data.

The putative substrate binding regions were identified and compared with those of other MCOs. This analysis was based on structural superimposition and the three-dimensional coordinates of *T. versicolor* laccase, a high-resolution structure recently solved in the presence of complexed substrate (36). This analysis revealed four loop regions, designated loops I, II, III, and IV, responsible for substrate binding specificity (Fig. 1). The MCO1 sequence was compared with the structural alignment, and the structural loop regions mapped to the primary sequence of this protein. High sequence variability was observed in all these regions of the selected proteins, and the MCO1 loops were generally larger than the other regions (Table l).

Sequence analysis of substrate binding loops. The sequence variation within the four substrate binding loops was analyzed independently for each class of the MCOs. A set of nonredundant protein sequences was selected from laccases, ascorbate oxidases, and ferroxidases, and a multiple alignment was constructed for each class of proteins. The MCO1 sequence was aligned with each multiple alignment, and the loop regions were identified (Table 2). These alignments revealed substantial similarity between loops III and IV of MCO1 and the corresponding regions in ferroxidases, whereas loop I of MCO1 most closely resembled the ascorbate oxidase sequence. Loop II of MCO1 had certain residues in common with ascorbate oxidases, and other loops had residues in common with ferroxidases. Overall, the analysis of substrate binding loops suggested that MCO1 is more closely related to ferroxidases and perhaps ascorbate oxidases than to the laccases.

Additional features are common to MCO1 and ferroxidases. MCO1 residue Glu-214, equivalent to Glu-185 of *Saccharomyces cerevisiae* Fet3, is not present in ascorbate oxidases and laccases and has been shown to be essential for ferroxidase activity (7). Other residues shared by the MCO1 and Fet3 proteins but absent in ascorbate oxidases and laccases include Glu-179, Glu-214, Pro-217, Gly-253, and Asn-455, while Thr-244 and Asp-457 are also absent in laccases but present in ascorbate oxidases. Despite the significant homology with Fet3 family members, MCO1 lacks the COOH-terminal transmembrane domain common to ferroxidases (12).

Heterologous expression of *mco1*. To obtain large quantities of protein for biochemical characterization, *mcol* cDNA was expressed in *A. nidulans* under control of the *A. oryzae* TAKA amylase promoter. Following enzymatic assays, transformants with consistently high activity were selected for further analysis. Cultures in *Aspergillus* minimal medium containing 5% maltose exhibited a maximum of 2.94 U of extracellular ferroxidase activity per ml on day 3 (equivalent to 0.2 U of laccase activity per ml as determined with ABTS), and the activity declined slowly up to day 6. The final yields were close to 30 mg/liter of culture. The enzymatic activity was similar when medium containing 0.5% yeast extract and 5% maltose supplemented with 100 μM $CuSO_4$ was used.

Enzyme purification and characterization. Purification of rMCO1 with Q-Sepharose yielded approximately 6 mg of a purified enzyme with a molecular mass of 78 kDa per liter of culture (Fig. 2). During fractionation, the presence of the enzyme was monitored by its blue color. Zymograms conducted in SDS-polyacrylamide gels under nonreducing conditions revealed the presence of only one major band with strong oxidase activity (Fig. 2). The purified rMCO1 (2 mg/ml) had the distinctive UV-visible absorbance spectra associated with type I (606 nm) and type III (330 nm) copper centers, con-

TABLE 1. Structural alignment of substrate binding loops in MCOs and the predicted MCO1 protein[a]

Protein[b]	Loop I[c]	Loop II	Loop III	Loop IV
Ascorbate oxidase 1AOZ	^{152}QEVGLSSKPIRWIGEPQ^{168}	^{280}VGTRARH---PN — TP— ----PG^{292}	^{353}QNVINGY VKWA^{363}	^{433}N ANMMKENLSET^{444}
Laccases				
1KYA	^{159}G--PA------FPLGAD^{166}	^{261}ANPN------FG---NV-GFTGGIN^{275}	^{332}FNG-----TNFF^{338}	^{386}A-TAAA---PGAP^{393}
1A65	^{159}I--Q------GAA-QPD^{165}	^{260}AQPN------KGRNGLAGTFANGVN^{278}	^{335}FSG-----GRFT^{341}	^{389}A-GV-----LGGP^{394}
1GW0	^{183}LVHFTQ — NNAPPFSD^{196}	^{290}VTFGGQAACGGS — LN--PH — P^{306}	^{363}LDLTGTPLFVWK^{374}	^{421}N DPEGP--FSLP^{430}
1GYC	^{159}G·· PR------FPLGAD^{166}	^{261}ANPN····· FG··· TV-GFAGGIN^{275}	^{332}FN-----GTNFF^{338}	^{386}A-TALA---PGAP^{393}
MCO1	^{196}LNAQYLSPSGPIGGSAG^{212}	^{310}TLQQ····· TDMFTYKLPGQNPDN^{328}	^{387}FDNLPSGASRAY^{398}	^{448}VLDLVLENNDNGD^{460}

[a] Structures were optimally superimposed in three-dimensional space, and the variable regions were identified. Based on the structure of the PDB code 1KYA laccase, which was solved in the presence of a natural inducer at the substrate binding site, the subset of variable regions in close contact with the ligand was identified in all the structures. A subset of four variable loops was finally obtained. The structural alignment of the proteins (generated after optimal superimposition of all the structures) was aligned with the MCO1 sequence which allowed mapping of the four variable structural regions in contact with the ligand to the MCO1 protein sequence.

[b] All known structures of MCOs were obtained from the PDB (4).

Primary sequences of selected loops, along with the sequential numbering of the Ranking residues, are show for all MCOs with known structures and MCO1.

TABLE 2. Sequence alignment of substrate binding loops in MCOs[a]

Protein	Loop I	Loop II	Loop III	Loop IV
Laccases				
Phanerocaete chrysosporium MCO1	LNAQYLSPSGPIGGSA	TLQQTDMFTYKLPGQNPD-N	FDNLPSGASRAYM	VLDLVLENNDNGD
Cryptococcus neoformans Lac	IIAALATPEGYKGNIA	T--SVA-LSCMFGAVSQE-G	-NVLGNTFQGYGF	---T-VI---D--
Cucumis cinereus Lac	-IPA---P-SIQG--A	AQPNKG-RNGLAGTFANGVN	--QLGFSGGRFTI	---AGVL---GGP
Trametes villosa Lcc3	-TPA------PL----	ANPNRANTTGFANGI----N	----TFNGSEFFI	---GGVT---GGP
Ceriporiopsis subvermispora Lcs-1	-AAA-----STLT--F	ANPNNG-NMGFANGI----N	----TFNGTNLFI	---GNII---AGP
Agaricus bisporus Lcc-1	-ILAPDATNEFFSSGI	A-PMTGGNPDRNPNLNISLT	---AQPNAPFFDI	---G------EGA
Thanatephorus cucumeris Lac4	-VLEKQMFSTNNTALL	A-PMTVAGAGTNANLDPTNV	-RSTVDGILRFTF	---HHR----GAD
Cryptococcusparasiticus Lac	-TAD--ELVVYTQSNA	VTFGGGGFCGKSNNPY---P	----STTTRKWTI	---ATGN---ALP
Pleurotus ostreatus Pox1	-VVA-------PQNAV	ADPNLG-STGFDGGI----N	--AFDVTNFELTI	---ALAV---GGP
Trametes versicolor Lac3	-VAA------NVGPAF	ANPNFG-NVGFTGGI----N	----NFNGTNFFI	---ATAA-APGAP
Trametes versicolor Lcc2	-TAA------RLGPRF	ANPNFG-TVGFAGGI----N	----NFNGTNFFI	---ATAL-APGAP
Nicotiana tabacum Lac	-TEAVINEAIKSGLA-	ASPFMDAPIAVDNVT----A	MPTVALLQAHFFG	---DTGIIAPEN-
Melanocarpus albomyces Lac	-RAA-DDLVHFTQNNA	VTFGGQAACGGSLNPH---P	-DLTGTPLFVWKV	---EGPF---SLP
Class	----------	----------	----------	--------XX---
All	----------	----------	----------	----------
Ascorbate oxidases				
Phanerochaete chrysosporium MCO1	LNAQY**L**-**S**-**P**SGP**IG**GSAG	TLQQTDMFTYK**L**PGQ**N**PDN	FDNLPSGASRAY	VLDLVLENNDNGD
Cucurbita pepo LaoZ	QEVG-**LSSKP**IRW**IG**EPQ-	TRARHPNTPPG**L**TLL**N**YLP	LPPTPYLGAMKY	QNANMMKENLSET
Arabidopsis thaliana AOZ	QELA-**LSSRP**MRW**IG**EPQ-	VRGREPKTPQA**L**TVI**N**YVD	VPVTPYLGSIRY	QNANVLKGVISEI
Cucurbita melo AOZ	QEVG-**LKSNP**MRW**IG**ELQ-	VRGRKPKTSPA**L**LLF**N**YLP	LPSTPYLGAIKF	QNANALTNNTSEI
Medicago truncatula AOZ	QEVG-**LSSAP**MRW**IG**EPQ-	VRGRKPSTPQA**L**TIL**N**YKP	LPTTPYLGSIKF	QNANQLNGNGSEI
Nicotiana tabacum AOZ	QEVD-**LSSNP**LRW**IG**EPQ-	VRGREPKTPQG**L**TLL**N**YLP	LPTQLYLGSIRY	QNANALAKDVSEI
Class	XX---X-X-X-XXXXX-X-	-X-X-X-X---X---XX--	-X---XXX----	XXXX------XX-
All	-----O-O-O---OO----	----------O---O----------		----------
Ferroxidases				
Phanerochaete chrysosporium MCO1	L-NAQYLSPSG**P**IGGSA	TLQQTDMFTYKL**P**GQNPD**N**	FDN**L**PS**G**ASR**A**Y	VLDLVLE**NN**D**N**G**D**
Neurospora crassa Fet3	L-QPRFMSKYNP----T	ASMDTTLFDT-I**P**PGLNT**N**	MNN**L**AS**G**ANY**A**F	IVQIVLN**N**L**D**S**G**R
Arrula adeninivorans Fet3	LNKEEFLTLYN**P**----T	SIFDENLFDV-I**P**SDLGM**N**	MTN**L**DN**G**VNY**A**F	WEIVVN**N**N**D**A**G**F
Saccharomyces cerevisiae Fet3	L-IPNFMSRFN**P**----T	QRVDDTMLDV-I**P**KDLEL**N**	MDN**L**DD**G**VNY**A**F	VIEIVLN**N**L**D**T**G**K
Schizocaccharomyces pombe Fet3	LVPDEFKTWKN**P**----T	AYMDESLFDT-I**P**DNYNP**N**	FFT**L**GD**G**ANY**A**E	WDVIID**N**H**D**T**G**K
Candida albicans Fet3	I-GPAFLTRFN**P**----T	NGVDTTMLDS-V**P**ADLQV**N**	MNV**L**ND**G**INY**A**F	IVDIVLN**NF**D**T**G**K**
Saccharomyces cerevisiae Fet3	L-TKSFMSVYN**P**----T	QKFDDTMLDV-I**P**SDLQL**N**	MDN**L**KN**G**VNY**A**F	IVEIVLN**NQ**D**T**G**T**
Class	-----X----XX----X	---X----X---X-----X	---X--X-XXX-	-------X-X-X-
All	----------O-----	----------O-----O	---O--O---O-	-------O-O-O-

[a] Within each class of MCOs (laccases, ascorbate oxidases, and ferroxidases), a subset of sequences, excluding close protein homologues, was selected and aligned. Multiple alignments containing the selected sequences for each class were independently realigned with the MCO1 sequence. The MCO1 regions predicted to be in contact with the substrate ligand (Table 1) were mapped in these multiple alignments, which allowed identification of the corresponding regions in laccases, ascorbate oxidases, and ferroxidases. For each protein class, conserved identical residues within the group of selected sequences are indicated by X. Residues conserved in each group and in the MCO1 sequence are indicated by boldface type and by **O** in the alignment.

firming the presence of these centers, as originally inferred from the deduced protein sequence (data not shown). When rMCO1 was analyzed by isoelectric focusing, six defined isoforms with oxidase activity were observed. The PIS of the bands ranged from 3.5 to 4.3. Due to the strong absorption of the type I copper, it was possible to identify some of the isoforms (Fig. 3).

Oxidase activity. Different compounds were tested as rMCO1 substrates. All three enzymes oxidized the aromatic amines 1,4-phenyldiamine and *o*-dianisidine. However, compared to the activities of laccase 51002 and rLcs1, phenolic compounds, such as cathecol, 2,6-dimethoxyphenol, and guiacol, were relatively poor substrates for rMCO1 (Table 3). Oxidation of 2,6-dimethoxyphenol and syringaldazine, substrates routinely oxidized by laccases, also occurred at low levels or was undetectable. The optimum pH for rMCO1 oxidation of ABTS was 3.0, which is similar to the optimum pHs of other laccases. The K_m for ABTS was 0.74 mM, which is 10- to 20-fold higher than the K_m values for most laccases. In contrast to some bacterial MCOs (17,18), rMCO1 could not oxidize MnII (data not shown). rMCO1 clearly differed from laccase

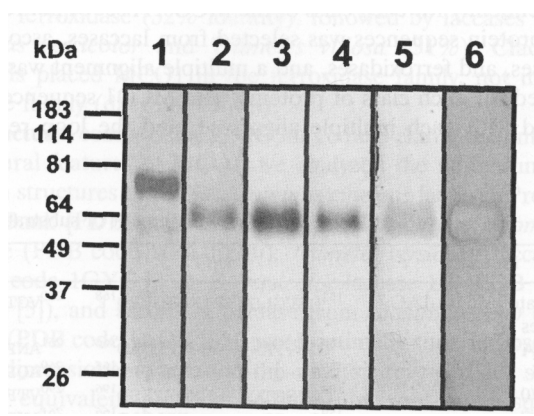

FIG. 2. Zymogram of rMCO1. Two-microgram portions of enzyme obtained after fractionation in Q-Sepharose, either treated with ß-mercaptoethanol (lane 1) or untreated (lanes 2, 3, 4, and 5), were subjected to SDS-polyacrylamide gel electrophoresis. The proteins were stained with Coomassie blue (lanes 1 and 2), stained for oxidase activity with ABTS (lane 3) or *o*-dianisidine (lane 4), stained for ferroxidase activity directly with Fe^{2+} (lane 5), or negatively stained with batophenanthroline-disulfonic acid (lane 6).

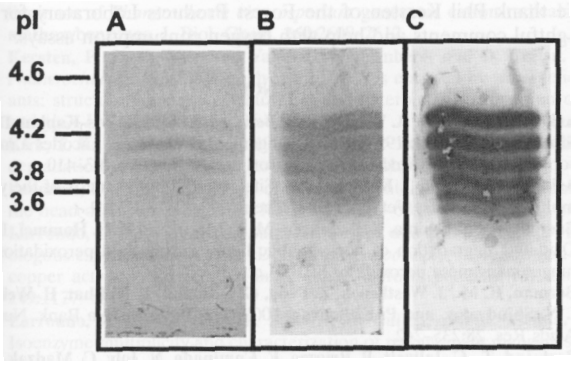

FIG. 3. Isoelectric focusing of rMCO1. (A) Direct visualization of 40 μg (0.25 U) of rMCO1 from the Q-Sepharose pool. (B and C) rMC01 (0.04 U) was stained with Coomassie blue (B) or developed with 1,8-diaminonaphtalene (C) as described in Materials and Methods. Units were defined with ABTS.

51002 and rLcs1 in the high level of activity observed with Fe^{2+} (Table 3).

Ferroxidase activity. rMCO1 oxidation of Fe^{2+} followed typica1 Michaelis-Menten kinetics (9) (data not shown). The ferroxidase activity of rMCO1 was inhibited >90% by 1 mM EDTA or 1 mM sodium azide. After incubation for 1 h at 60°C, the enzyme retained 55% of its activity. The optimum pH, as measured with sodium acetate as the buffer, was 3.4 (data not shown). To allow comparison with Fet3, all kinetic parameters were determined at pH 5. The K_m and k_{cat} for Fe^{2+} oxidation were about 2.05 μM and 2,450 min^{-1}, respectively. This K_m is considerably lower than the values obtained for oxidation of aromatic substrates, which fell in the millimolar range (data not shown). In aggregate, rMCO1 more closely resembles a ferroxidase than a laccase.

DISCUSSION

Lignin-degrading fungi secrete various oxidative enzymes, including LiP, MnP, and laccase. Some species produce all three enzymes, other species produce two of the enzymes, and some apparently produce only one enzyme (23). Laccase and MnP activities are easily measured in cultures of efficient lignin degraders, such as *C. subvermispora* and *Phanerochaete sordida.* No LiP activity has been detected in cultures of these fungi, yet inexplicably, LiP-like sequences have been PCR amplified from the genomes of both species (38). Another white rot fungus, *P. cinnabarinus,* produces only laccases, and mutants deficient in this enzyme are unable to degrade lignin (15). Peroxidized lipids (3, 25) and low-molecular-weight compounds (10) have been implicated as mediators in the attack of nonphenolic residues by MnP and laccase, respectively.

For many years, the conventional view was that *P. chrysosporium* produces only LiP and MnP (16, 23, 28, 44). More recently, however, in several reports workers have described low laccase activity under culture conditions that differ from those typically employed. These conditions include high concentrations of nitrogen and copper (39), the use of cellulose instead of glucose as a carbon source (42), and growth in semisolid cultures (13). However, it has been suggested that laccase identification based on ABTS oxidation may be misleading due to an artifact caused by Mn^{3+} (37).

In this work, we searched the *P. chrysosporium* genome database and identified four sequences with homology to MCOs, all of which were clustered in a 25-kb region. In addition, a gene encoding a membrane-anchored ferroxidase, highly homologous to *S. cerevisiae fet3,* was identified at a separate locus. Of all the MCO genes, only *mco1* featured a predicted secretion signal. Comparisons of MCO1 to fungal laccases revealed all of the histidine and cysteine residues that participate in copper binding, but the overall sequence similarity was low.

MCO1 has several characteristics that are unique for an MCO. In some regions it shares residues with ascorbate oxidases but not with laccases, while other segments have some similarity to laccases but not to ascorbate oxidases. MCO1 also has significant similarity to Fet3 proteins, especially with the ferroxidase from *Arxula adeninivorans* (48). Together with iron permease Ftr1 (43), Fet3 plays a key role in iron homeostasis. Interestingly, *Cryptococcus* neoformans laccase also has some iron oxidase activity (32, 50), shares certain structural features with ferroxidases (Table 2), and belongs to the same group as MCO1 (data not shown).

Based on structural alignments, MCO1 has substantial homology with Fet3 proteins but not with laccases in several regions close to the copper centers, such as loops III and IV (Table 2). High levels of sequence divergence of laccases in the four loops might explain their extended substrate range.

Several studies have focused on identification of the structural determinants that confer ferroxidase activity on MCOs (2, 7, 8). Glu-185 and Tyr-354 are essential for the oxidation of Fe^{2+} by Fet3 from *S. cerevisiae.* These two residues are conserved in all known Fet3 proteins and are absent in ascorbate oxidases and laccases, including the *C. neoformans* laccase. MCO1 has the equivalent Glu-185 residue but has an Arg-396 residue instead of a Tyr-354 residue, suggesting that Glu-185, but not Tyr-354, is essential for Fe^{2+} oxidation. However, it is possible that Tyr-398 could serve the function normally served by Tyr-354. Like all ferroxidases that have been described, MCO1 has a Leu residue as the P4 ligand for type I copper,

TABLE 3. Substrate specificities of rMCO1, laccase from *C. subvermispora,* and laccase 51002

Compound	Oxygen consumption (nmol/min)[a]		
	rMCOl	Laccase 51002	rLcs1
Fe^{2+}	39	8.6	4.6
o-Dianisidine	23	35	28
p-Anisidine	9.0	5.1	9.2
1,4-Phenyldiamine	52	37	23
2,6-Dimethoxyphenol	5.1	52	23
Syringaldazine	0	28	12
ABTS	3.2	52	21
Guaiacol	1.8	44	17
Gallic acid	4.6	32	7.4
Phloroglucinol	0	15	1.9
Pyrogallol	5.5	52	12
Resorcinol	1.1	4.4	1.8

[a] Averages for triplicate assays performed with 1 μg of enzyme in 0.1 mM acetate buffer (pH 5.0). In most cases the substrate concentration was 1 mM; the concentration of syringaldazine used was 0.1 mM.

while most laccases have a Phe residue and most ascorbate oxidases have a Met residue at this position.

The *mco1* cDNA was expressed in *A. nidulans*, and the corresponding protein was characterized. In vitro assays with several substrates and a characteristic spectrum confirmed that *mco1* encodes an MCO. The deduced molecular mass of the enzyme was 59.1 kDa, which is 75.7% of the experimentally determined molecular mass (78 kDa). The difference could be partially attributed to N glycosylation, because treatment with endoglycosidase decreased the apparent size approximately 10 kb (data not shown). Assuming that digestion of N-glycans was complete, the difference in molecular mass could be attributed to 0-linked glycans. The predicted and observed molecular masses of MCO1 are similar to those of numerous fungal laccases (44), all of which are rather different from laccases found in cultures of *P. chrysosporium* (i.e., 100 kDa [42] and 46.5 kDa [13]).

The substrate specificity of rMCO1 is different from that of previously described laccases. The oxidation of commonly used laccase substrates, such as 2,6-dimethoxyphenol, syringaldazine, and ABTS, was substantially less with rMCOl than with the *C. subvermispora* enzyme or the commercial product (Table 3). With ABTS, perhaps the most widely used laccase substrate, the K_m of rMCO1 was almost 10-fold higher than the values for most laccases. Other phenolic compounds also were poor substrates. In contrast, rMCOl had a high level of ferroxidase activity, with a K_m on the same order of magnitude as that described for Fet3 (11). In addition, considerable oxidase activity with aromatic amines was observed, a property common among Fet3 proteins (7, 11). On the other hand, the optimum pH of rMCO1 (pH 3.4) is lower than the optimum pHs of Fet3 family members, which are near pH 5.0 (11). In short, MCO1 is a novel fungal MCO with a strong ferroxidase activity but lacks the canonical domains of Fet3 proteins.

The substrate specificity of MCOl suggests a possible role in regulating reactive oxygen species. It is well-known that the oxidation of Fe^{2+} by H_2O_2 leads to production of hydroxyl radicals through the Fenton reaction ($Fe^{2+} + H_2O_2$ ® $Fe^{3+} + OH^- + {}^{\cdot}OH$). These highly reactive radicals nonspecifically attack all wood polymers and are probably the main agents that cause rapid cellulose depolymerization by brown rot fungi. An unanswered question has been how white rot fungi modulate Fenton reactions, which might otherwise result in toxic levels of hydroxyl radicals. *mcol* and three other genes with potential ferroxidase activity in *P. chrysosporium* may play a role in modulating Fe^{2+} availability. A similar function was proposed for *C. neoformans* laccase (32, 50).

In summary, both structural and biochemical data suggest that MCOl is a new type of MCO that shares some features with laccases and Fet3 proteins. We are now measuring the expression of *mco1* in *P. chrysosporium* under different cultural conditions and determining what role, if any, this enzyme has in lignocellulose degradation.

ACKNOWLEDGMENTS

This work was financed by grants 8990004, 1010959, and 2000076 from FONDECYT-Chile, by the Millenium Institute for Fundamental and Applied Biology, Chile, and by U.S. Department of Energy grant DE-FG02-87ER13712. L.F.L is a predoctoral fellow supported by Fundacion Andes,

We thank Phil Kersten of the Forest Products Laboratory for his thoughtful comments and help with oxygen consumption assays.

REFERENCES

1. **Askwith, C., D. Eide, A. Van Ho, P. S. Bernard, L. Li, S. Davis-Kaplan, D. M. Sipe, and J. Kaplan.** 1994. The *FET3* gene of *S. cerevisiae* encodes a multicopper oxidase required for ferrous iron uptake. Cell 76403410.
2. **Askwith, C. C., and J. Kaplan.** 1998. Site-directed mutagenesis of the yeast multicopper oxidase Fet3p. J. Biol. Chem. **273:**22415–22419.
3. **Bao, W., Y. Fuknshima, K. A. Jensen, M. A. Moen, and K. E. Hammel.** 1994. Oxidative degradation of non-phenolic lignin during lipid peroxidation by fungal manganese peroxidase. FEBS Lett. **354:**297–300.
4. **Berman, H. M., J. Westbrook, Z. Feng, G. Gilliland, T. N. Bhat, H. Weissig, I. N. Shindyalov, and P. E. Bourne.** 2000. The Protein Data Bank. Nucleic Acids Res. **28:**235–242.
5. **Bertrand, T., C. Jolivalt, P. Briozzo, E. Caminade, N. Joly, C. Madzak, and C. Mongin.** 2002. Crystal structure of a four-copper laccase complexed with an arylamine: insights into substrate recognition and correlation with kinetics. Biochemistry **41:**7325–7333.
6. **Blanchette, R.** 1991. Delignification by wood-decay fungi. Annu. Rev. Phytopathol. **29:**381–398.
7. **Bonaccorsi di Patti, M. C., M. R. Felice, A. P. Camuti, A. Lania, and G. Musci.** 2000. The essential role of Glu-185 and Tyr-354 residues in the ferroxidase activity of *Saccharomyces cerevisiae* Fet3. FEBS Lett. **472:**283–286.
8. **Bonaccorsi di Patti, M. C., M. P. Paronetto, V. Dolci, M. R. Felice, A. Lania, and G. Musci.** 2001. Mutational analysis of the iron binding site of *Saccharomyces cerevisiae* ferroxidase Fet3. An in vivo study. FEBS Lett. **508:**475–478.
9. **Bonomi, F., D. M. Kurtz, and X. Cui.** 1996. Ferroxidase activity of recombinant *Desulfovibrio vulgaris* rubrerythrin. J. Biol. Inorg. Chem. **1:**67–72.
10. **Bourhonnais, R., and M. G. Paice.** 1990. Oxidation of non-phenolic substrates. An expanded role for laccase in lignin biodegradation. FEBS Lett. **267:**99–102.
11. **de Silva, D., S. Davis-Kaplan, J. Fergestad, and J. Kaplan.** 1997. Purification and characterization of Fet3 protein, a yeast homologue of ceruloplasmin. J. Biol. Chem. **272:**14208–14213,
12. **De Silva, D. M., C. C. Askwith, D. Eide, and J. Kaplan.** 1995. The FET3 gene product required for high affinity iron transport in yeast is a cell surface ferroxidase. J. Biol. Chem. 2701098–1101.
13. **Dittmer, J., N. Patel, S. Dhawale, and S. Dhawale.** 1997. Production of multiple laccase forms by *Phanerochaete chrysosporium* grown under nutrient sufficiency. FEMS Microbiol. Lett. **149:**65–70.
14. **Ducros, V., A. M. Brzozowski, K. S. Wilson, S. H. Brown, P. Ostergaard, P. Schneider, D. S. Yaver, A. H. Pedersen, and G. J. Davies.** 1998. Crystal structure of the type-2 Cu-depleted laccase from *Coprinus cinereus* at 2.2 A resolution. Nat. Struct. Biol. **5:**310–316.
15. **Eggert, C., U. Temp, and K. Eriksson.** 1997. Laccase is essential for lignin degradation by the white-rot fungus *Pycnoporus cinnabarinus.* FEBS Lett. **407:**89–92.
16. **Eriksson, K.-E. L., R. A. Blanchette, and P. Ander.** 1990. Microbial and enzymatic degradation of wood and wood components. Springer-Verlag, Berlin, Germany.
17. **Francis, C. A., E. M. Co, and B. M. Tebo.** 2001. Enzymatic manganese(II) oxidation by a marine alpha-proteobacterinm. Appl. Environ. Microbiol. **67:**40244029.
18. **Francis, C. A., and B. M. Tebo.** 2002. Enzymatic manganese(II) oxidation by metabolically dormant spores of diverse *Bacillus* species. Appl. Environ. Microbiol. **68:**874–880.
19. **Gilliland, G., S. Perrin, and H. Bunn.** 1990. Competitive PCR for quantitation of mRNA, p. 60–69. *In* M. Innis, D. Gelfand, J. Sninsky, and T. White (ed.), PCR protocols. Academic Press, New York, N.Y.
20. **Hakulinen, N., L. L. Kiiskinen, K. Kruus, M. Saloheimo, A. Paananen, A. Koivula, and J. Rouvinen.** 2002. Crystal structure of a laccase from *Melanocarpus albomyces* with an intact trinuclear copper site. Nat. Struct. Biol. **9:**601-605.
21. **Hammel, K. E., B. Kalyanaraman, and T. K. Kirk.** 1986. Substrate free radicals are intermediates in ligninase catalysis. Proc. Natl. Acad. Sci. USA **83:**3808–3812.
22. **Harvey, P. J., H. E. Schoemaker, R. M. Bowen, and J. M. Palmer.** 1985. Single-electron transfer processes and the reaction mechanism of enzymic degradation of lignin. FEBS Lett. **183:**13–16.
23. **Hatakka, A.** 1994. Lignin-modifying enzymes from selected white-rot fungi: production and role in lignin degradation. FEMS Microbiol. Rev. **13:**125–135.
24. **Horton, R., H. Hunt, S. Ho, J. Pullen, and L. Pease.** 1989. Engineering hybrid genes without the use of restriction enzymes: gene splicing by overlap extension. Gene **77:**61–68.
25. **Kapich, A. N., K. A. Jensen, and K. E. Hammel.** 1999. Peroxyl radicals are potential agents of lignin biodegradation. FEBS Lett. **461:**115–119.
26. **Kersten, P. J., M. Tien, B. Kalyanaraman, and T. K. Kirk.** 1985. The

ligninase of *Phanerochaete chrysosporium* generates cation radicals from methoxybenzenes. J. Biol. Chem. **260:**2609–2612.

27. **Kersten, P. J., C. Witek, A. Vanden Wymelenberg, and D. Cullen.** 1995. *Phanerochaete chrysosporium* glyoxal oxidase is encoded by two allelic variants: structure, genomic organization and heterologous expression of *glx1* and *glx2*. J. Bacteriol. **177:**6106–6110.
28. **Kirk, T. K., and R. L. Farrell.** 1987. Enzymatic "combustion": the microbial degradation of lignin. Annu. Rev. Microbiol. **41:**465–505.
29. **Laemmli, U. K.** 1970. Cleavage of structural proteins during the assembly of the head of bacteriophage T4. Nature **227:**2680–685.
30. **Larrondo, L. F., M. Avila, L. Salas, D. Cullen, and R. Vicuna.** 2003. Heterologous expression of laccase cDNA from *Ceriporiopsis subvermispora* yields copper activated apoprotein and complex isoform patterns. Microbiology **149:** 1177-1182.
31. **Larrondo, L. F., S. Lobos, P. Stewart, D. Cullen, and R Vicuna.** 2001. Isoenzyme multiplicity and characterization of recombinant manganese peroxidases from Ceriporiopsis *subvermispora* and *Phanerochaete chrysosporium.* Appl. Environ. Microbiol. **67:**2070–2075.
32. **Liu, L., R. P. Tewari, and P. R. Williamson.** 1999. Laccase protects *Cryptococcus neoformans* from antifungal activity of alveolar macrophages. Infect. Immun. **67:**6034–6039.
33. **Lobos, S., J. Larrain, L. Salas, D. Cullen, and R. Vicuna.** 1994. Isozymes of manganese-dependent peroxidase and laccase produced by the lignin-degrading basidiomycete *Ceriporiopsis subvermispora.* Microbiology **140:**2691–2698.
34. **Marquez, L., H. Wariishi, H. B. Dunford, and M. H. Gold.** 1988. Spectroscopic and kinetic properties of oxidized intermediates of lignin peroxidase from *Phanerochaete chrysosporium.* J. Biol. Chem. **263:**10549–10552.
35. **Messerschmidt, A., R. Ladenstein, R Huber, M. Bolognesi, L. Avigliano, R. Petruzzelli, A. Rossi, and A. Finazzi-Agro.** 1992. Refined crystal structure of ascorbate oxidase at 1.9 A resolution. J. Mol. Biol. **224:**179–205.
36. **Piontek, K., M. Antorini, and T. Choinowski.** 2002. Crystal structure of a laccase from the fungus *Trametes versicolor* at 1.90-A resolution containing a full complement of coppers. J. Biol. Chem. **277:**37663–37669.
37. **Podgornik, H., M. Stegu, E. Zibert, and A. Perdih.** 2001. Laccase production by *Phanerochaete chrysosporium*—an artifact caused by Mn(III)? Lett. Appl. Microbiol. **32:**407-411.
38. **Rajakumar, S., J. Gaskell, D. Cullen, S. Lobos, E. Karahanian, and R. Vicuna.** 1996. Lip-like genes in *Phanerochaete sordida* and *Ceriporiopsis subvermispora,* white rot fungi with no detectable lignin peroxidase activity. Appl. Environ. Microbiol. **62:**2660–2663.
39. **Rodriguez, C. S., R. Santro, C. Cameselle, and A. Sanroman.** 1997. Laccase production in semi-solid cultures of *Phanerochaete chrysosporium.* Biotechnol. Lett. **19:**995–998.
40. **Sali, A., and T. L. Blundell.** 1993. Comparative protein modelling by satisfaction of spatial restraints. J. Mol. Biol. **234:**779–815.
41. **Schoemaker, H. E., P. J. Harvey, R. M. Bowen, and J. M. Palmer.** 1985. On the mechanism of enzymatic lignin breakdown. FEBS Lett. **183:**7–12.
42. **Srinivasan, C., T. D'Sonza, K. Boominathan, and C. Reddy.** 1995. Demonstration of laccase in the white rot basidiomycete *Phanerochaete chrysosporium* BKM-F-1767. Appl. Environ. Microbiol. **61:**4274-4277.
43. **Stearman, R., D. S. Yuan, Y. Yamaguchi-Iwai, R. D. Klausner, and A. Dancis.** 1996. A permease-oxidase complex involved in high-affinity iron uptake in yeast. Science **271:**1552–1557.
44. **Thurston, C. F.** 1994. The structure and function of fungal laccases. Microbiology **140:**19–26.
45. **Vallim, M. A., B. J. Janse, J. Gaskell, A. A. Pizzirani-Kleiner, and D. Cullen.** 1998. *Phanerochaete chrysosporium* cellobiohydrolase and cellobiose dehydrogenase transcripts in wood. Appl. Environ. Microbiol. **64:**1924–1928.
46. **Wariishi, H., L. Akileswaran, and M. H. Gold.** 1988. Manganese peroxidase from the basidiomycete *Phanerochaete chrysosporium:* spectral characterization of the oxidized states and the catalytic cycle. Biochemistry **27:**5365–5370.
47. **Wariishi, H., and M. H. Gold.** 1990. Lignin peroxidase compound III. Mechanism of formation and decomposition. J. Biol. Chem. **265:**2070–2077.
48. **Wartmann, T., U. W. Stephan, I. Bube, E. Boer, M. Melzer, R. Manteuffel, R. Stoltenbnrg, L. Guengerich, G. Gellissen, and G. Kunze.** 2002. Post-translational modifications of the AFET3 gene product: a component of the iron transport system in budding cells and mycelia of the yeast *Arxula adeninivorans.* Yeast **19:**849–862.
49. **Williams, D. M., G. R. Lee, and G. E. Cartwright.** 1974. Ferroxidase activity of rat ceruloplasmin. Am. J. Physiol. **227:**1094–1097.
50. **Williamson, P. R.** 1994. Biochemical and molecular characterization of the diphenol oxidase of *Cryptococcus neoformans:* identification as a laccase. J. Bacteriol. **176:**656–664.
51. **Wymelenberg, A. V., S. Denman, D. Dietrich, J. Bassett, X. Yu, R. Atalla, P. Predki, U. Rudsander, T. T. Teeri, and D. Cullen.** 2002. Transcript analysis of genes encoding a family 61 endoglucanase and a putative membrane-anchored family 9 glycosyl hydrolase from *Phanerochaete chrysosporium.* Appl. Environ. Microbiol. **68:**576.5–5768.